Communications of BAO, Vol. 70, Issue 1, 2023, pp. 106-113

Cosmological Scalar Field ϕCDM Models

Olga Avsajanishvili *

E.Kharadze Georgian National Astrophysical Observatory, 47/57 Kostava St.,Tbilisi 0179, Georgia

Abstract

Cosmological models that go beyond the standard Lambda Cold Dark Matter (ΛCDM) scenario, namely, scalar field ϕCDM models, are considered. The Hubble expansion rate of the universe, the dynamic and the energetic domination of dark energy, the formation of matter density fluctuations and the large-scale structure growth rate in these models compared to the standard spatially-flat ΛCDM model are investigated.

Keywords: *dark energy, scalar field, Hubble expansion rate, large-scale structure growth rate.*

1. Introduction

Our universe is expanding with an acceleration according to reliable observational datasets: measurements of Supernovae type Ia magnitudes (Perlmutter et al., 1999, Riess et al., 1998), measurements of the temperature anisotropy and the polarization in the cosmic microwave background (CMB) radiation (Bennett et al., 1996, Smoot et al., 1992), examining of the large-scale structure of the universe (Dodelson et al., 2001, Percival et al., 2007) measurements of baryon acoustic oscillations peak length scale (Blake et al., 2011, Eisenstein et al., 2005) measurements of the Hubble parameter (Stern et al., 2010).

One of the possible explanations for this empirical fact is that the energy density of the universe is dominated by so-called dark energy, a component with an effective negative pressure (Copeland et al., 2006, Peebles & Ratra, 2003).

The simplest description for dark energy is the concept of vacuum energy or the time-independent cosmological constant Λ, first introduced by Albert Einstein (Einstein, 1915a,b). The cosmological model based on such a description of dark energy in the spatially flat universe is called the standard, concordance or fiducial Lambda Cold Dark Matter (ΛCDM) model. In the ΛCDM model, the general theory of relativity describes the gravity in the universe on large scales. The energy density associated with the cosmological constant is 68.5% of the total energy density of the universe at present (Aghanim et al., 2020).

Being still a fiducial cosmological model at present, the ΛCDM model has several still unsolved problems, the number of which increases as more accurate observational data are obtained (Abdalla et al., 2022, Di Valentino et al., 2019). The main of which are the fine tuning or the cosmological constant problem, the coincidence problem, the Hubble parameter tension problem, the parameter S_8 tension problem, the problem of the shape of the universe, and the preference for observational data of dynamical dark energy (in particular, phantom dark energy) (Abdalla et al., 2022, Aghanim et al., 2020, Di Valentino et al., 2019, 2021).

The presence of all the above discrepancies of the ΛCDM model is interpreted as a crisis of modern cosmology (Di Valentino et al., 2019). Although some of them may be due to systematic errors, their persistence strongly points to the need for new physics and new cosmological models that go beyond the standard ΛCDM scenario, on the one hand, and on tensions and anomalies in the current CMB data, on the other (Di Valentino, 2022).

The main alternative to the ΛCDM model are dynamical scalar field ϕCDM models (Ratra & Peebles, 1988a,b, Wetterich, 1988). In these models, dark energy is represented in the form of a slowly varying uniform cosmological scalar field at present. This family of models avoids the coincidence problem of the ΛCDM model. In these models, the energy density and the pressure are time dependent functions under the assumption that the scalar field is described by the ideal barotropic fluid model.

*olga.avsajanishvili@iliauni.edu.ge

doi: https://doi.org/10.52526/25792776-23.70.1-106

In general, dynamical dark energy models are characterized by the equation of state (EoS) parameter w_ϕ, which is the ratio of the pressure p_ϕ to the energy density p_ϕ: $w_\phi = p_\phi/\rho_\phi$. If for the ΛCDM model, the EoS parameter is a constant and equals minus one, then for ϕCDM models, the EoS parameter is a time-dependent function. Dynamical dark energy can mimic the cosmological constant at present, while becoming almost indistinguishable from it. These models are divided into phantom models (Caldwell, 2002) and quintessence models (Caldwell & Linder, 2005, Peebles & Ratra, 2003). These two classes of models differ from each other: (i) by the range of values of the EoS parameter at present epoch: this is $-1 < w_0 < -1/3$ for the quintessence field, and $w_0 < -1$ for the phantom field; (ii) by the sign of the kinetic term in the Lagrangian: positive for the quintessence field, and negative for the phantom field; (iii) by the form of the Klein-Gordon scalar field equation of motion; (iv) by the dynamics of scalar fields: the quintessence field rolls gradually to the minimum of its potential, while the phantom field rolls to the maximum of its potential; (v) by the temporal evolution of dark energy: for the quintessence field, the dark energy density remains almost unchanging with time, while it increases for the phantom field; (vi) by forecasting the future of the universe: depending on the spatial curvature of the universe, quintessence models predict either an eternal expansion of the universe, or a repeated collapse. On the other hand, phantom models predict the destruction of any gravitationally-related structures in the universe.

This paper is organized as follows: models under study are presented in Section 2, results and discussions are considered in Section 3, conclusions are summarized in Section 4.

We applied the natural system of units, where $c = k_B = 1$.

2. Models

We considered two types of scalar field ϕCDM models in the spatially flat universe: the quintessence and phantom scalar field ϕCDM models. The flat, homogeneous and isotropic universe is described by the Friedmann-Lemaître-Robertson-Walker spacetime metric $ds^2 = -dt^2 + a(t)^2 d\mathbf{x}^2$, where t is the cosmic time and $a(t)$ is the scale factor (normalized to be unity at present epoch $a_0 \equiv a(t_0)$).

The action for quintessence and phantom scalar field ϕCDM models are, respectively

$$S = \frac{M_{pl}^2}{16\pi} \int d^4x \Big[\sqrt{-g}\Big(\pm \frac{1}{2} g^{\mu\nu} \partial_\mu\phi\partial_\nu\phi - V(\phi)\Big)\Big], \tag{1}$$

here M_{pl} is a Planck mass, the "+/−" sign before kinetic term corresponds to the quintessence/phantom model, the over-dot denotes a derivative with respect to the cosmic time, $g^{\mu\nu}$ is the metric tensor, $g \equiv \det(g^{\mu\nu})$ is the determinant of the metric tensor $g^{\mu\nu}$, and $V(\phi)$ is the self-interacting potential of the scalar field ϕ.

2.1. Quintessence scalar field Ratra-Peebles ϕCDM model

We studied the quintessence scalar field ϕCDM model with the inverse power law Ratra-Peebles potential (Ratra & Peebles, 1988a), which has a form

$$V(\phi) = \frac{1}{2}\kappa M_{\rm pl}^2 \phi^{-\alpha}, \tag{2}$$

where $\alpha > 0$ and $\kappa > 0$ are model parameters. The model parameter α defines the steepness of this potential, for $\alpha = 0$, the ϕCDM model reduces to the ΛCDM model. We considered values of the parameter α in the range $0 < \alpha \leq 0.7$, according to observations (Samushia, 2009). The form of the quintessence Ratra-Peebles potential in 3D space is presented in the left panel of Fig. 1.

The Klein–Gordon scalar field equation of motion and the normalized Hubble parameter for the quintessence scalar Ratra-Peebles field ϕCDM model read, respectively, as

$$\ddot{\phi} + 3\frac{\dot{a}}{a}\dot{\phi} - \frac{1}{2}\kappa\alpha M_{\rm pl}^2 \phi^{-(\alpha+1)} = 0, \tag{3}$$

$$E(a) = H(a)/H_0 = \Big(\Omega_{\rm r0} a^{-4} + \Omega_{\rm m0} a^{-3} + \frac{1}{12H_0^2}\Big(\dot{\phi}^2 + \kappa M_{\rm pl}^2 \phi^{-\alpha}\Big)\Big)^{1/2}, \tag{4}$$

where $H(a) = \frac{\dot{a}}{a}$ is a Hubble expansion rate of the universe; H_0 is a Hubble constant $H_0 = 100h$ km c^{-1} Mpc^{-1}, with h is a dimensionless normalized Hubble constant; $\Omega_{\rm r0}$ is a radiation density parameter at present epoch,

doi: https://doi.org/10.52526/25792776-23.70.1-106

$\Omega_{\rm m0}$ is a matter density parameter at present epoch. We fixed values of parameters $\Omega_{m0} = 0.315$, $h = 0.674$ to the best-fit values obtained by Planck collaboration (Aghanim et al., 2020).

The dark energy density parameter Ω_ϕ and the matter density parameter $\Omega_{\rm m}$ are defined, respectively, as

$$\Omega_\phi = \frac{1}{12H_0^2}\Big(\dot\phi^2 + \kappa M_{\rm pl}^2\phi^{-\alpha}\Big), \qquad \Omega_{\rm m} = \frac{\Omega_{\rm m0}a^{-3}}{\Omega_{\rm r0}a^{-4} + \Omega_{\rm m0}a^{-3} + \frac{1}{12H_0^2}\Big(\dot\phi^2 + \kappa M_{\rm pl}^2\phi^{-\alpha}\Big)}. \tag{5}$$

The energy density ρ_ϕ, the pressure p_ϕ and the EoS parameter w_ϕ for the quintessence scalar field Ratra-Peebles ϕCDM model are of the form, respectively

$$\rho_\phi = \frac{M_{\rm pl}^2}{32\pi}\Big(\dot\phi^2 + \kappa M_{\rm pl}^2\phi^{-\alpha}\Big), \quad p_\phi = \frac{M_{\rm pl}^2}{32\pi}\Big(\dot\phi^2 - \kappa M_{\rm pl}^2\phi^{-\alpha}\Big), \quad w_\phi = \frac{p_\phi}{\rho_\phi} = \frac{\dot\phi^2 - \kappa M_{\rm pl}^2\phi^{-\alpha}}{\dot\phi^2 + \kappa M_{\rm pl}^2\phi^{-\alpha}}. \tag{6}$$

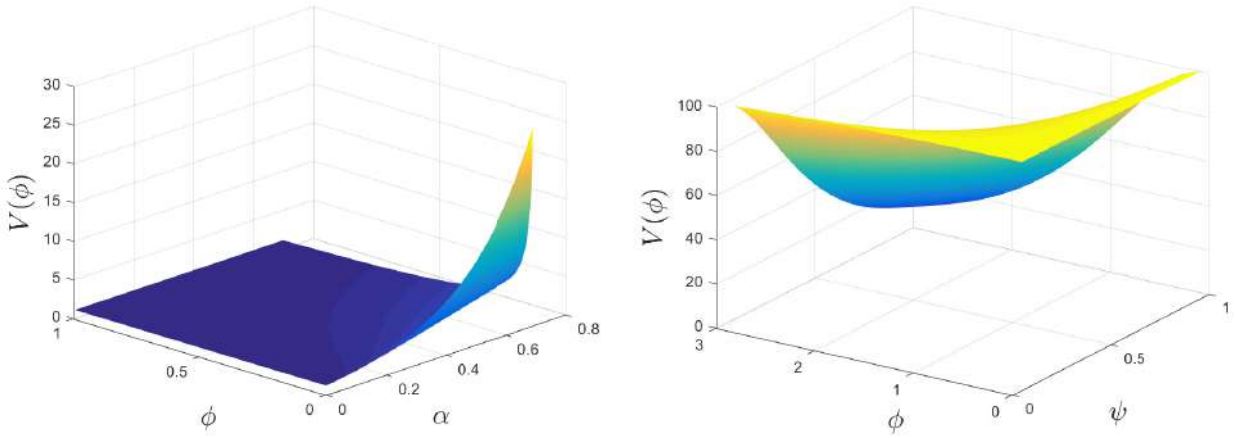

Figure 1. The form of the quintessence Ratra-Peebles potential $V(\phi) \sim \phi^{-\alpha}$ in 3D space, in units $M_{\rm pl} = 1$ (left panel). The form of the phantom inverse hyperbolic cosine potential $V(\phi) \sim \cosh(\psi\phi)^{-1}$ in 3D space (right panel).

2.2. Phantom scalar field inverse hyperbolic cosine ϕCDM model

We also studied the phantom scalar field ϕCDM model with the inverse hyperbolic cosine potential $V(\phi) = V_0\cosh^{-1}(\psi\phi)$ (Rakhi & Indulekha, 2009), where $\psi > 0$ and $V_0 > 0$ are model parameters. In the right panel of Fig. 1 is shown the form of the phantom inverse hyperbolic cosine potential in 3D space.

The Klein–Gordon scalar field equation of motion and the normalized Hubble parameter for the phantom inverse hyperbolic cosine scalar field ϕCDM model are given, respectively, as

$$\ddot\phi + 3\frac{\dot a}{a}\dot\phi - V_0\psi\tanh(\psi\phi)\cosh^{-1}(\psi\phi) = 0, \tag{7}$$

$$E(a) = H(a)/H_0 = \Big(\Omega_{\rm r0}a^{-4} + \Omega_{\rm m0}a^{-3} + \frac{1}{6H_0^2}\Big(-\frac{\dot\phi^2}{2} + V_0\cosh^{-1}(\psi\phi)\Big)\Big)^{1/2}. \tag{8}$$

The dark energy density parameter Ω_ϕ and the matter density parameter $\Omega_{\rm m}$ are defined, respectively, as

$$\Omega_\phi = \frac{1}{6H_0^2}\Big(-\frac{\dot\phi^2}{2} + V_0\cosh^{-1}(\psi\phi)\Big), \qquad \Omega_{\rm m} = \frac{\Omega_{\rm m0}a^{-3}}{\Omega_{\rm r0}a^{-4} + \Omega_{\rm m0}a^{-3} + \frac{1}{12H_0^2}\Big(-\frac{\dot\phi^2}{2} + V_0\cosh^{-1}(\psi\phi)\Big)}. \tag{9}$$

The energy density ρ_ϕ, the pressure p_ϕ and the EoS parameter w_ϕ for the phantom inverse hyperbolic cosine scalar field ϕCDM model have the form, respectively

$$\rho_\phi = \frac{M_{\rm pl}^2}{16\pi}\Big(-\frac{\dot\phi^2}{2} + V_0\cosh^{-1}(\psi\phi)\Big), \quad p_\phi = \frac{M_{\rm pl}^2}{16\pi}\Big(-\frac{\dot\phi^2}{2} - V_0\cosh^{-1}(\psi\phi)\Big), \quad w_\phi = \frac{p_\phi}{\rho_\phi} = \frac{-\dot\phi^2/2 - V_0\cosh^{-1}(\psi\phi)}{-\dot\phi^2/2 + V_0\cosh^{-1}(\psi\phi)}. \tag{10}$$

doi: https://doi.org/10.52526/25792776-23.70.1-106

3. Results and discussion

3.1. Background in the universe for scalar field ϕCDM models

To study the background in the universe for scalar field ϕCDM models, we jointly numerically integrated the first Friedmann's equation and the Klein-Gordon scalar field equation of motion, namely, Eq. (3) and Eq. (4) for the quintessence Ratra-Peebles scalar field ϕCDM model, Eq. (7) and Eq. (8) for the phantom inverse hyperbolic cosine scalar field ϕCDM model.

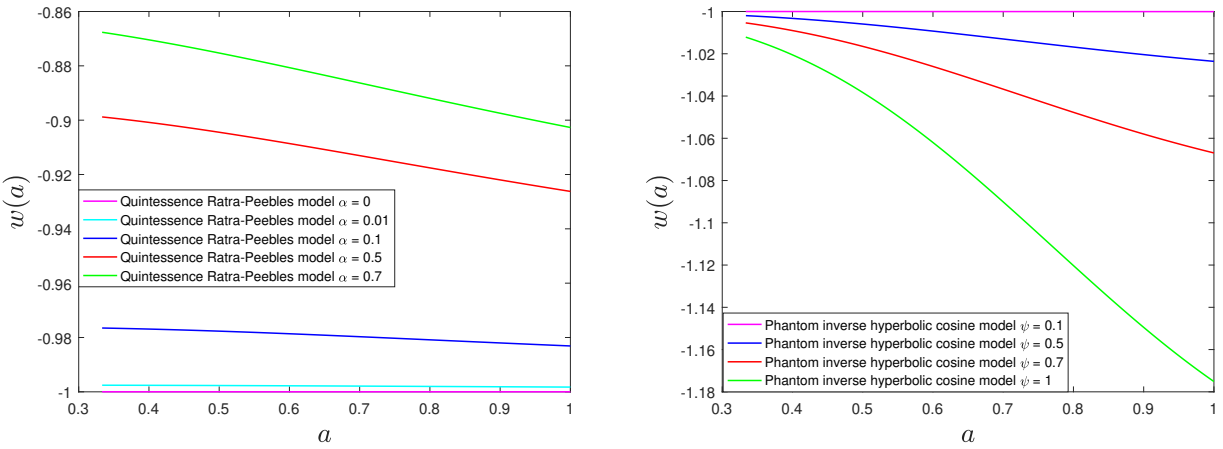

Figure 2. Dependence of the EoS parameter on the model parameter α in the quintessence Ratra-Peebles ϕCDM model (left panel). Dependence of the EoS parameter on the model parameter ψ in the phantom inverse hyperbolic cosine scalar field ϕCDM model (right panel).

The evolution of the EoS parameter for scalar field ϕCDM models depending on model parameters are presented in Fig. 2. A larger value of the parameter α in the quintessence Ratra-Peebles model (left panel of Fig. 2) and the parameter ψ in the phantom inverse hyperbolic cosine model (right panel of Fig. 2) causes an increase in dark energy and, thus, a stronger time dependence of the EoS parameter in these models and vice versa.

In order to study the influence of scalar fields on the Hubble expansion rate of the universe, we numerically calculated the Eq. (4) for the quintessence Ratra-Peebles ϕCDM model and Eq. (8) for the phantom inverse hyperbolic cosine scalar field ϕCDM model. The expansion rate of the universe is faster in quintessence scalar field ϕCDM models and slower in phantom scalar field ϕCDM models compared to the ΛCDM model (the left panel of Fig. 3).

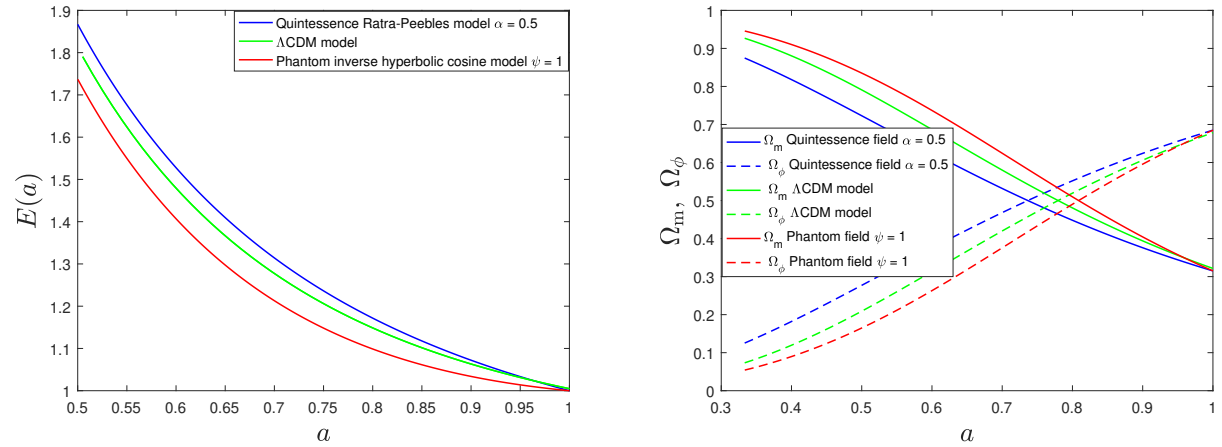

Figure 3. The evolution of the normalized Hubble expansion rate $E(a)$ in ϕCDM models for fixed values of model parameters compared to the ΛCDM model (left panel). The evolution of the matter density parameter $\Omega_{\rm m}$ and the dark energy density parameter Ω_ϕ in ϕCDM models for fixed values of model parameters compared to the ΛCDM model (right panel).

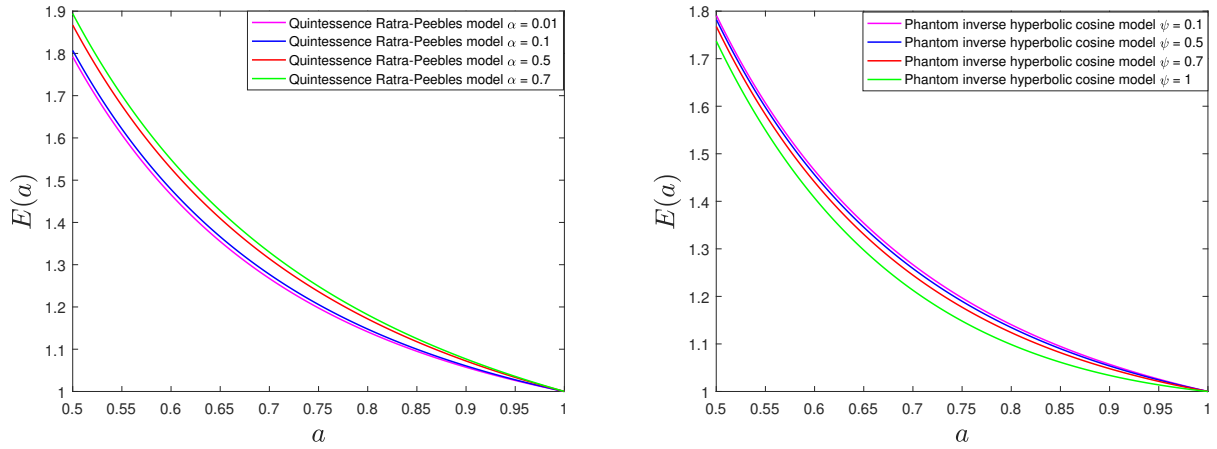

Figure 4. Dependence of the normalized Hubble expansion rate $E(a)$ on the model parameter α in the quintessence Ratra-Peebles ϕCDM model (left panel) and on the model parameter ψ in the phantom inverse hyperbolic cosine scalar field ϕCDM model (right panel).

In quintessence scalar field models, the Hubble expansion of the universe occurs faster with an increase in the value of the model parameter α (the left panel of Fig. 4), and, conversely, in phantom scalar field models, with an increase in the value of the model parameter ψ, the Hubble expansion of the universe occurs more slowly (the right panel of Fig. 4).

By investigating the influence of scalar fields on energy components in the universe, we found that the epoch of dominance of dark energy is established earlier in the quintessence Ratra-Peebles scalar field ϕCDM model and later in the phantom inverse hyperbolic cosine scalar fieldϕCDM model, compared to the ΛCDM model (the right panel of Fig. 3).

In the quintessence Ratra-Peebles scalar field ϕCDM model, the energetic domination of dark energy began earlier with an increase in the value of the model parameter α (the upper left panel of Fig. 5), and, conversely, in phantom scalar field models, with an increase in the value of the model parameter ψ, the energetic domination of dark energy began later (the upper right panel of Fig. 5). While the dynamic dominance of dark energy began earlier in the quintessence Ratra-Peebles scalar field ϕCDM model than in the phantom inverse hyperbolic cosine scalar field ϕCDM model (bottom panels of Fig. 5). Both in the quintessence and in the phantom scalar fields model, the dynamic dominance of dark energy began earlier than the energy dominance at the fixed values of model parameters in these models (Fig. 5).

3.2. The evolution of the large-scale structure in the universe for scalar field ϕCDM models

In order to study the influence of ϕCDM models on the formation of the large-scale structure in the universe, we numerically integrated the linear perturbation equation (Pace et al., 2010) relative to the matter density fluctuation δ

$$\delta'' + \left(\frac{3}{a} + \frac{E'}{E}\right)\delta' - \frac{3\Omega_{m0}}{2a^5E^2}\delta = 0. \tag{11}$$

We also calculated the linear growth factor $D(a) = \delta(a)/\delta(a_0)$ and the large-scale structures growth rate $f(a) = d\ln D(a)/d\ln a$.

The evolution of the linear growth factor $D(a)$ in ϕCDM models for fixed values of model parameters are presented in the left panel of Fig. 6. Larger values of matter density fluctuations are generated in quintessence scalar field ϕCDM models and smaller ones in phantom scalar field ϕCDM models, compared to the ΛCDM model (the left panel of Fig. 6). The large-scale structure growth rate $f(a)$ is slower in quintessence scalar fields, but faster in phantom scalar fields compared the ΛCDM model (the right panel of Fig. 6), because the Hubble expansion is faster in quintessence scalar fields than in phantom scalar fields (the left panel of Fig. 3), which leads to suppression of the large-scale structure growth rate in the universe.

In the quintessence Ratra-Peebles scalar field ϕCDM model, the larger values of matter density fluctuations are generated with an increase in the value of the model parameter α (the upper left panel of Fig. 7), and, conversely, in the phantom inverse hyperbolic cosine scalar field ϕCDM model, the smaller

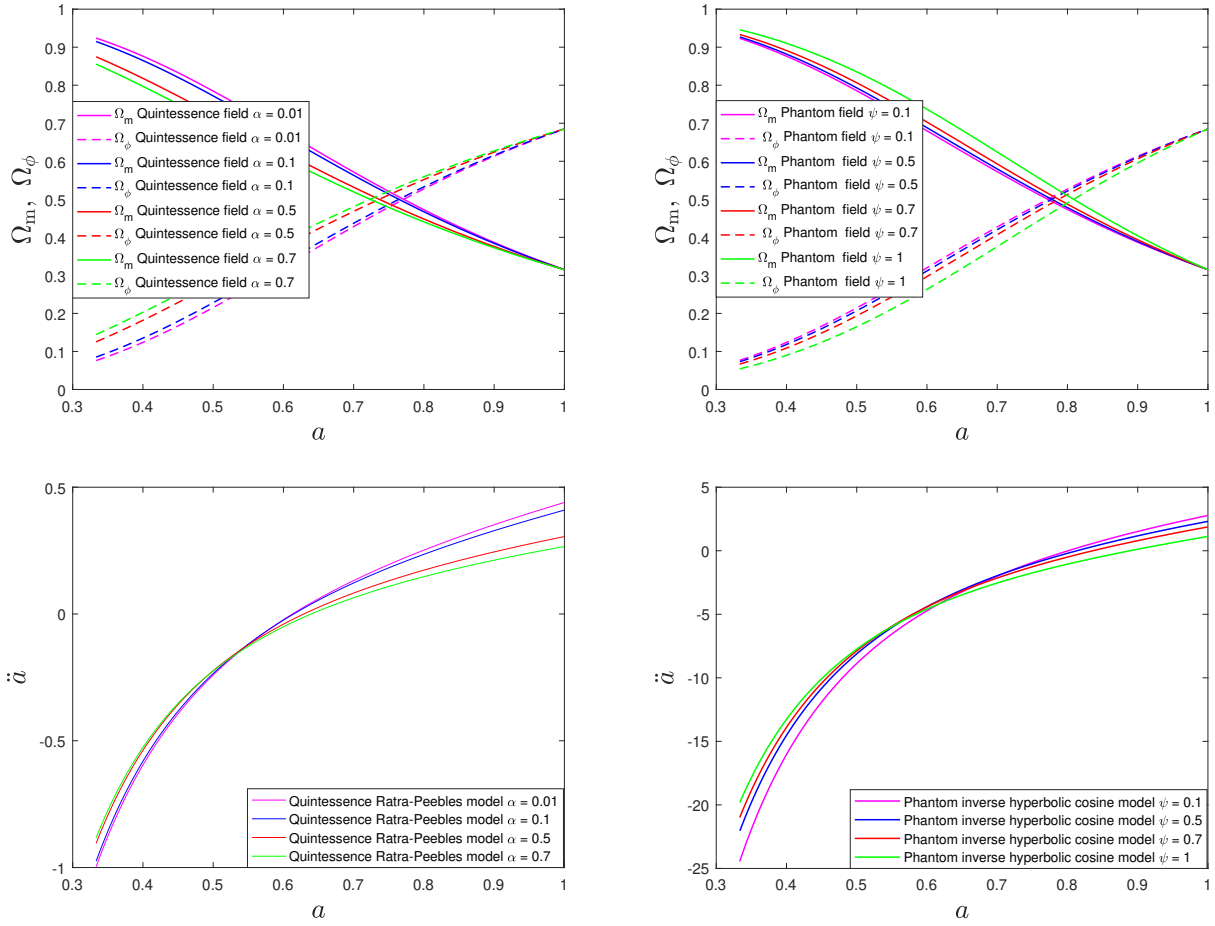

Figure 5. The energetic domination of dark energy in the quintessence Ratra-Peebles scalar field ϕCDM model depending on the model parameter α (upper left panel). The energetic domination of dark energy in the phantom inverse hyperbolic cosine scalar field ϕCDM model depending on the model parameter ψ (upper right panel). The dynamic domination of dark energy in the quintessence Ratra-Peebles scalar field ϕCDM model depending on the model parameter α (bottom left panel). The dynamic domination of dark energy in the phantom inverse hyperbolic cosine scalar field ϕCDM model depending on the model parameter ψ (bottom right panel).

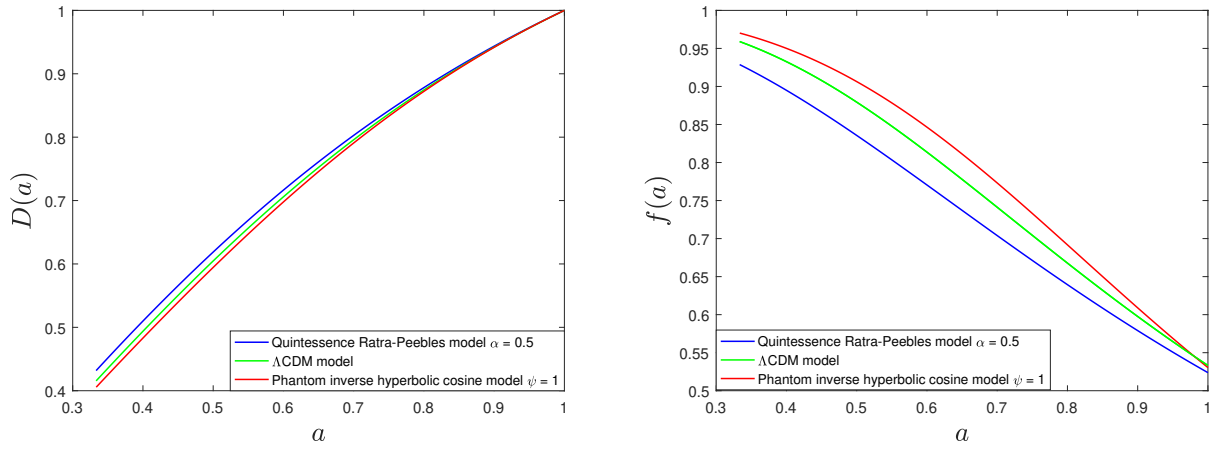

Figure 6. The evolution of the linear growth factor in ϕCDM models for fixed values of model parameters compared to the ΛCDM model (left panel). The evolution of the large-scale structure growth rate in ϕCDM models for fixed values of model parameters compared to the ΛCDM model (right panel).

values of matter density fluctuations are generated with an increase in the value of the parameter ψ (the upper right panel of Fig. 7). In the quintessence Ratra-Peebles scalar field ϕCDM model, the large-scale

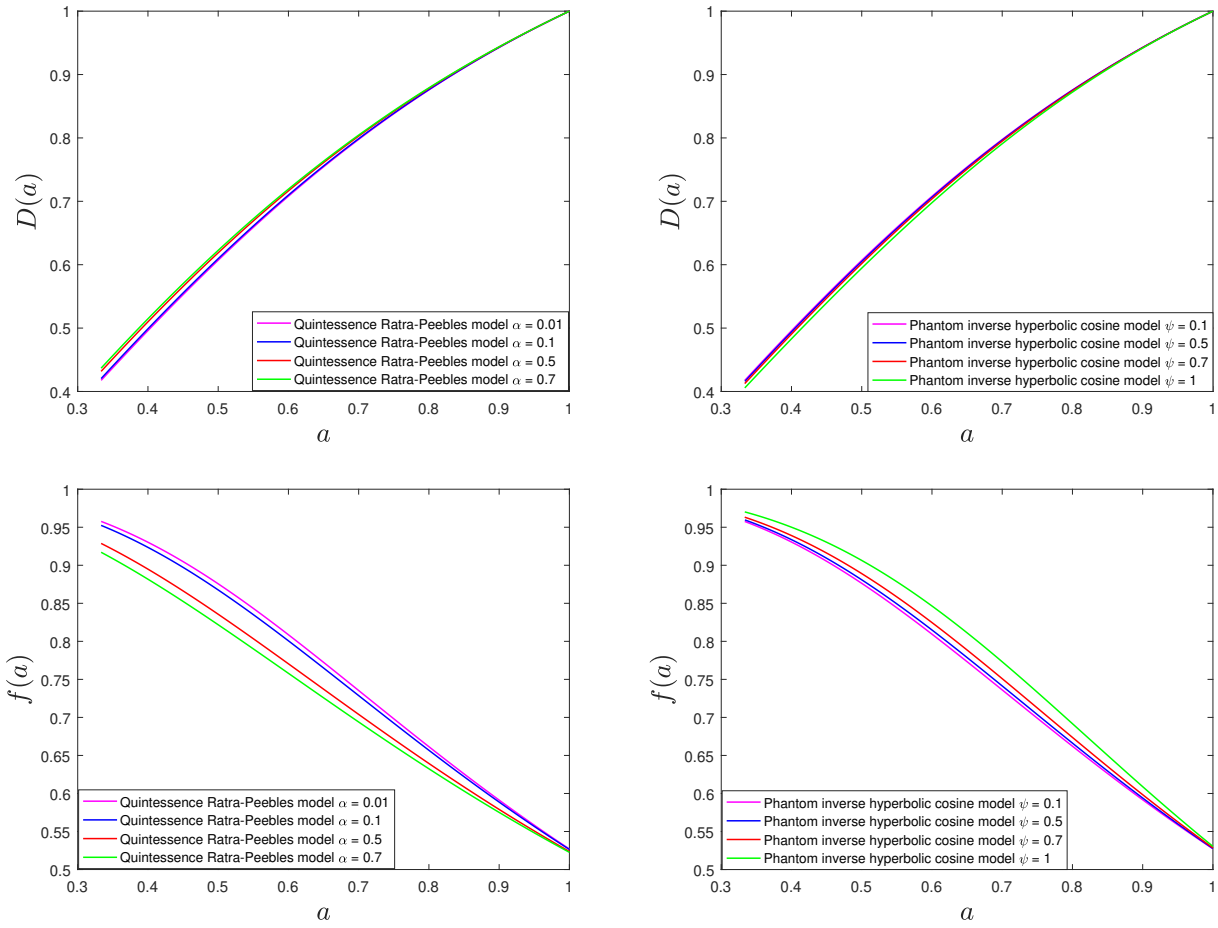

Figure 7. The evolution of the linear growth factor in the quintessence Ratra-Peebles scalar field ϕCDM model depending on the model parameter α (upper left panel). The evolution of the linear growth factor in the phantom inverse hyperbolic cosine scalar field ϕCDM model depending on the model parameter ψ (upper right panel). The evolution of the large-scale structures growth rate in the quintessence Ratra-Peebles scalar field ϕCDM model depending on the model parameter α (bottom left panel). The evolution of the large-scale structures growth rate in the phantom inverse hyperbolic cosine scalar field ϕCDM model depending on the model parameter ψ (bottom right panel).

structure growth rate $f(a)$ slows down with an increase in the value of the model parameter α (the bottom left panel of Fig. 7), and, conversely, in the phantom inverse hyperbolic cosine scalar field ϕCDM model, with an increase in the value of the parameter ψ, the large-scale structure growth rate rapids (the bottom right panel of Fig. 7).

4. Conclusions

Scalar field ϕCDM models differ from the ΛCDM model in a number of characteristics, which are generic for these models. Compared to the ΛCDM model:

- the Hubble expansion rate of the universe is faster in quintessence scalar field models and slower in phantom scalar field models;
- the dynamic and the energetic domination of dark energy began earlier in quintessence scalar field models and later in phantom scalar field models;
- larger values of matter density fluctuations are generated in phantom scalar field models and smaller ones in quintessence scalar field models;
- the large-scale structures growth rate of the universe is faster in phantom scalar field models and slower in quintessence scalar field models.

doi: https://doi.org/10.52526/25792776-23.70.1-106

Acknowledgements

This work was supported by Shota Rustaveli National Science Foundation of Georgia (SRNSFG) [YS-22-998].

References

Abdalla E., Abellán G. F., Aboubrahim A., et al. 2022, JHEAp, 34, 49

Aghanim N., Akrami Y., Ashdown M., et al. 2020, Astron. Astrophys. , 641, A6

Bennett C. L., Banday A., Gorski K. M., et al. 1996, Astrophys. J. Lett. , 464, L1

Blake C., Kazin E., Beutler F., et al. 2011, Mon. Not. R. Astron. Soc. , 418, 1707

Caldwell R. R., 2002, Phys. Lett., B545, 23

Caldwell R. R., Linder E. V., 2005, Phys. Rev. Lett., 95, 141301

Copeland E. J., Sami M., Tsujikawa S., 2006, Int. J. Mod. Phys., D15, 1753

Di Valentino E., 2022, Universe, 8, 399

Di Valentino E., Melchiorri A., Silk J., 2019, Nature Astron., 4, 196

Di Valentino E., Mena O., Pan S., et al. 2021, Class. Quant. Grav., 38, 153001

Dodelson S., Narayanan V. K., Tegmark M., et al. 2001, Astrophys. J. , 572, 140

Einstein A., 1915a, Sitzungsber. Preuss. Akad. Wiss. Berlin (Math. Phys.), 1915, 778

Einstein A., 1915b, Sitzungsber. Preuss. Akad. Wiss. Berlin (Math. Phys.), 1915, 844

Eisenstein D. J., Zehavi I., Hogg D. W., et al. 2005, Astrophys. J. , 633, 560

Pace F., Waizmann J.-C., Bartelmann M., 2010, Mon. Not. R. Astron. Soc. , 406, 1865

Peebles P. J. E., Ratra B., 2003, Rev. Mod. Phys., 75, 559

Percival W. J., Cole S., Eisenstein D. J., et al. 2007, Mon. Not. R. Astron. Soc. , 381, 1053

Perlmutter S., Aldering G., Goldhaber G., et al. 1999, Astrophys. J. , 517, 565

Rakhi R., Indulekha K., 2009, arXiv:0910.5406

Ratra B., Peebles P. J. E., 1988a, Astrophys. J. , 325, L17

Ratra B., Peebles P. J. E., 1988b, Phys. Rev., D37, 3406

Riess A. G., Filippenko A. V., Challis P., et al. 1998, Astron. J. , 116, 1009

Samushia L., 2009, PhD thesis, Kansas State U., arXiv:0908.4597

Smoot G. F., Bennett C. L., Kogut A., et al. 1992, Astrophys. J. Lett. , 396, L1

Stern D., Jimenez R., Verde L., et al. 2010, JCAP, 02, 008

Wetterich C., 1988, Nucl. Phys., B302, 645